Electronic Supplementary Material (ESI) for Polymer Chemistry.

Supporting Information for

Effect of Conjugated/Elastic block Sequence on Morphology and Electronic Properties of Polythiophene based Stretchable Block Copolymers

Yun-Chi Chiang,[1] Saburo Kobayashi,[2] Takuya Isono,[2] Chien-Chung Shih,[1] Tomoki Shingu,[2] Chih-Chien Hung,[3] Hui-Ching Hsieh,[1] Shih-Huang Tung,[3,4] Toshifumi Satoh,[,2] and Wen-Chang Chen[*,1,3,4]*

[1]Department of Chemical Engineering, National Taiwan University, Taipei 10617, Taiwan

[2]Faculty of Engineering and Graduate School of Chemical Sciences and Engineering, Hokkaido University. Sapporo 060-8628, Japan.

[3]Institute of Polymer Science and Engineering, National Taiwan University, Taipei 10617, Taiwan

[4]Advanced Research Center for Green Materials Science and Technology, National Taiwan University, Taipei 10617, Taiwan

Fabrication and Characterization of Field-Effect Transistors. FET transistors were fabricated with a bottom-gate/top-contact configuration. A 300 nm SiO_2 layer with capacitance per unit area = 10 nF cm^{-2} as gate dielectric was thermally grown onto the highly n-type doped Si (100) substrates. The substrates were modified with an octadecyltrimethoxysilane (ODTS) self-assembled monolayer. The polymer thin films were spin-casted onto modified SiO_2/Si substrates, and a post-annealing process at 150 °C under vacuum for 30 min was consequently introduced. The top-contact source/drain gold electrodes with thickness of 65 nm were thermally evaporated through a regular shadow mask, with the channel length (L) and width (W) being 50 and 1000 μm, respectively. The device characterizations were measured by using a Keithley 4200-SCS semiconductor parameter analyzer (Keithley Instruments Inc., Cleveland, OH) in a N_2-filled glove box.

1. Supplementary Tables

Table S1. Thermal properties of P3HT, POO and the studied block copolymers

	T_d[a] (°C)	T_g[b] (°C)	T_{m1}[b] (°C)	T_{m2}[b] (°C)	ΔH[c] (J/g)
P3HT	413	N.A.	N.A.	197.4	2.86
ABA	374	-66.4	-16.3	188.7	1.26
AB	361	-68.8	-15.8	188.8	1.31
BAB	358	-69.9	-15.0	190.1	1.40
POO	327	-74.0	-14.6	N.A.	N.A.

[a]Determined by thermal gravimetric analysis (TGA).

[b]Determined by differential scanning calorimetry (DSC).

[c]Integrated area from T_{m2} by differential scanning calorimetry (DSC).

Table S2. FET Characteristics of the studied block copolymers

	Mobility[a] ($cm^2V^{-1}s^{-1}$)	On/off ratio[a]	V_{TH}[a] (V)
ABA	2.6×10^{-4}	4.0×10^{3}	-10.3
AB	1.3×10^{-4}	7.7×10^{3}	-3.9
BAB	7.7×10^{-5}	3.8×10^{3}	-0.8

[a]The electrical properties are averaged from at least 5 devices of 2 batches.

2. Supplementary Figures

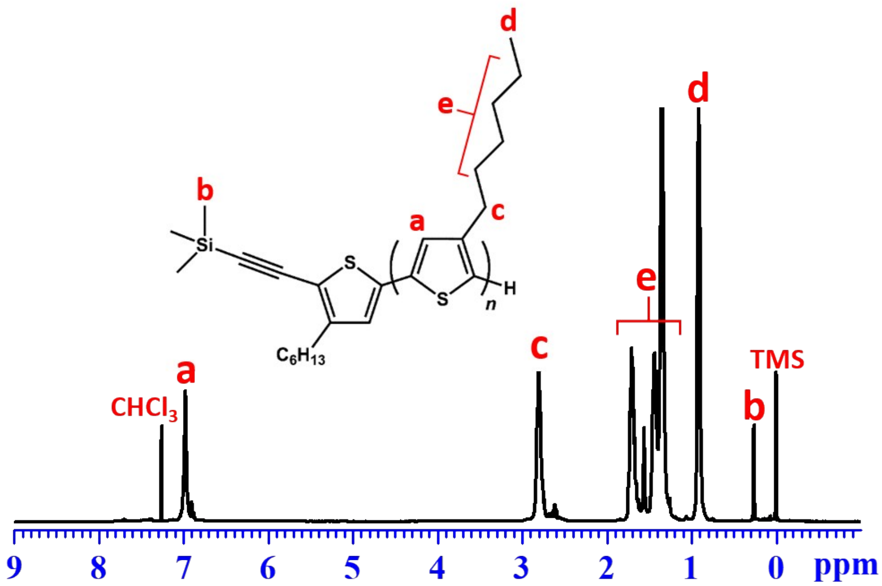

Figure S1. ^{1}H NMR spectrum of α-P3HT$_{32}$.

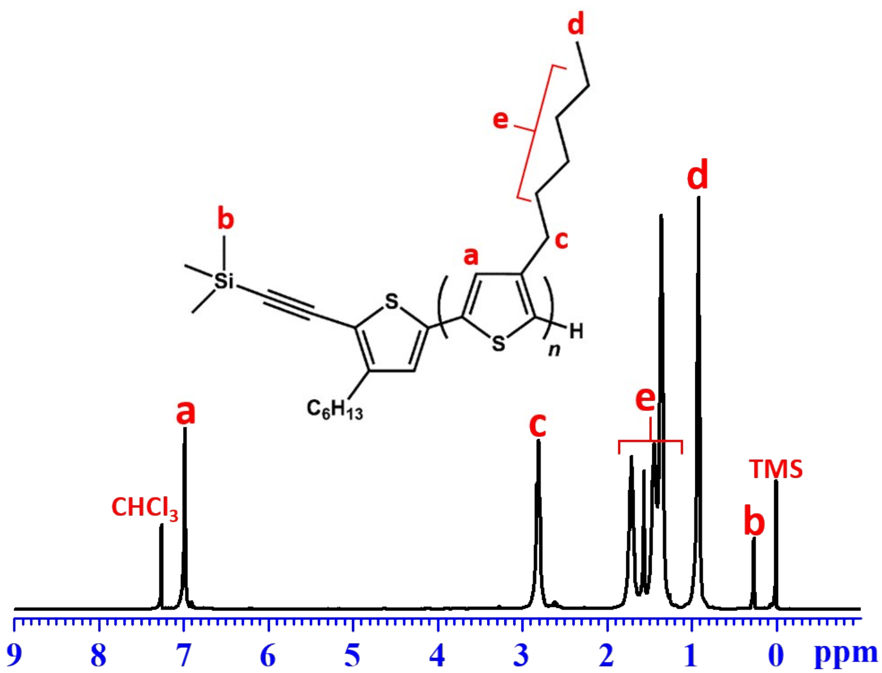

Figure S2. ^{1}H NMR spectrum of α-P3HT$_{37}$.

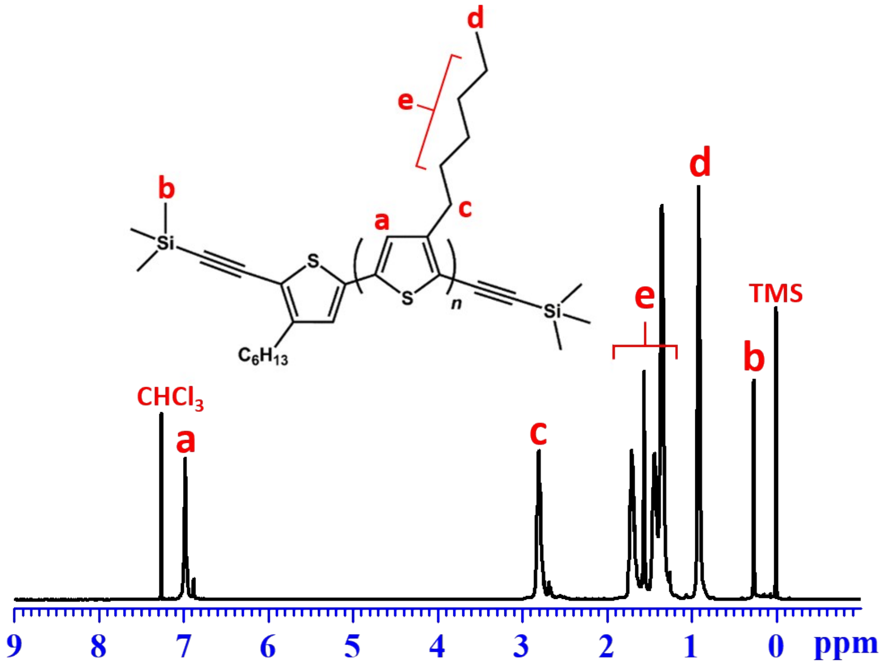

Figure S3. ^{1}H NMR spectrum of *α, ω*-P3HT$_{37}$.

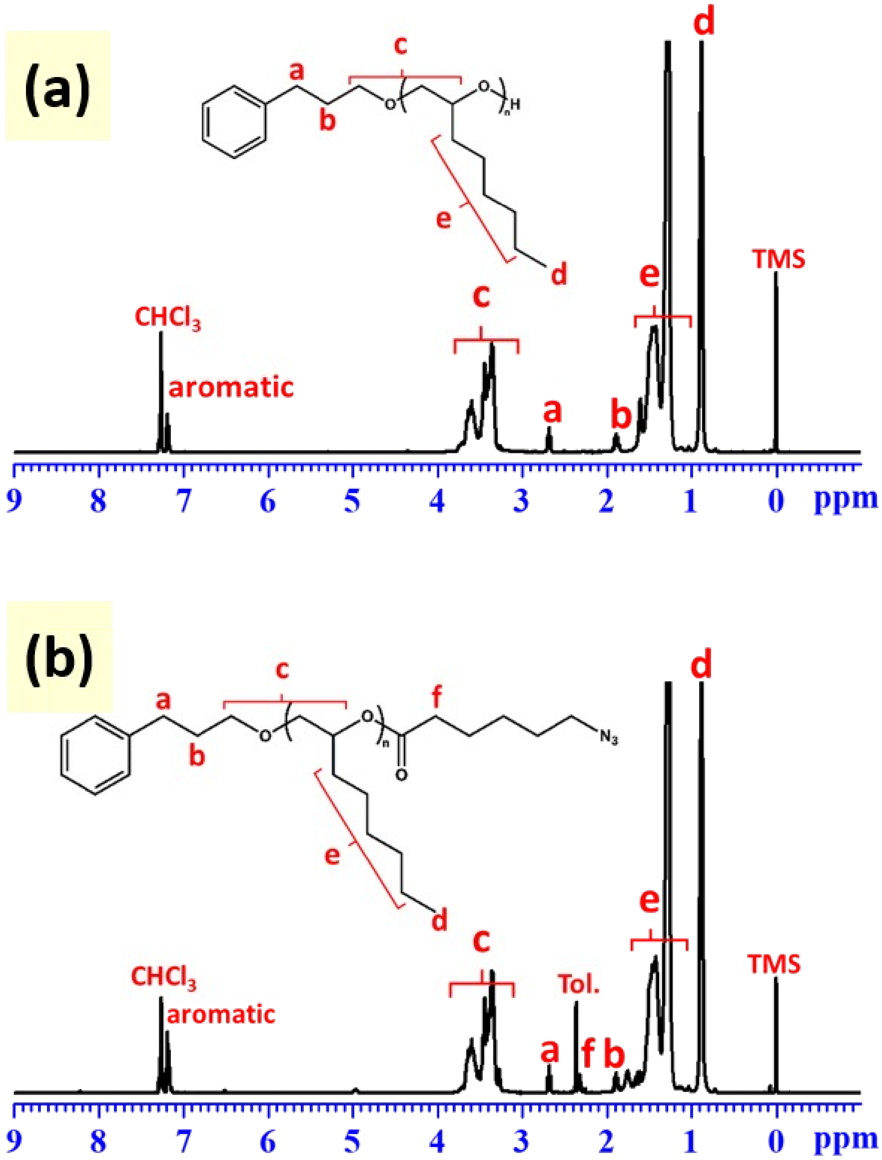

Figure S4. ^{1}H NMR spectrum of (a) POO_{16} and (b) POO_{16}-N_3.

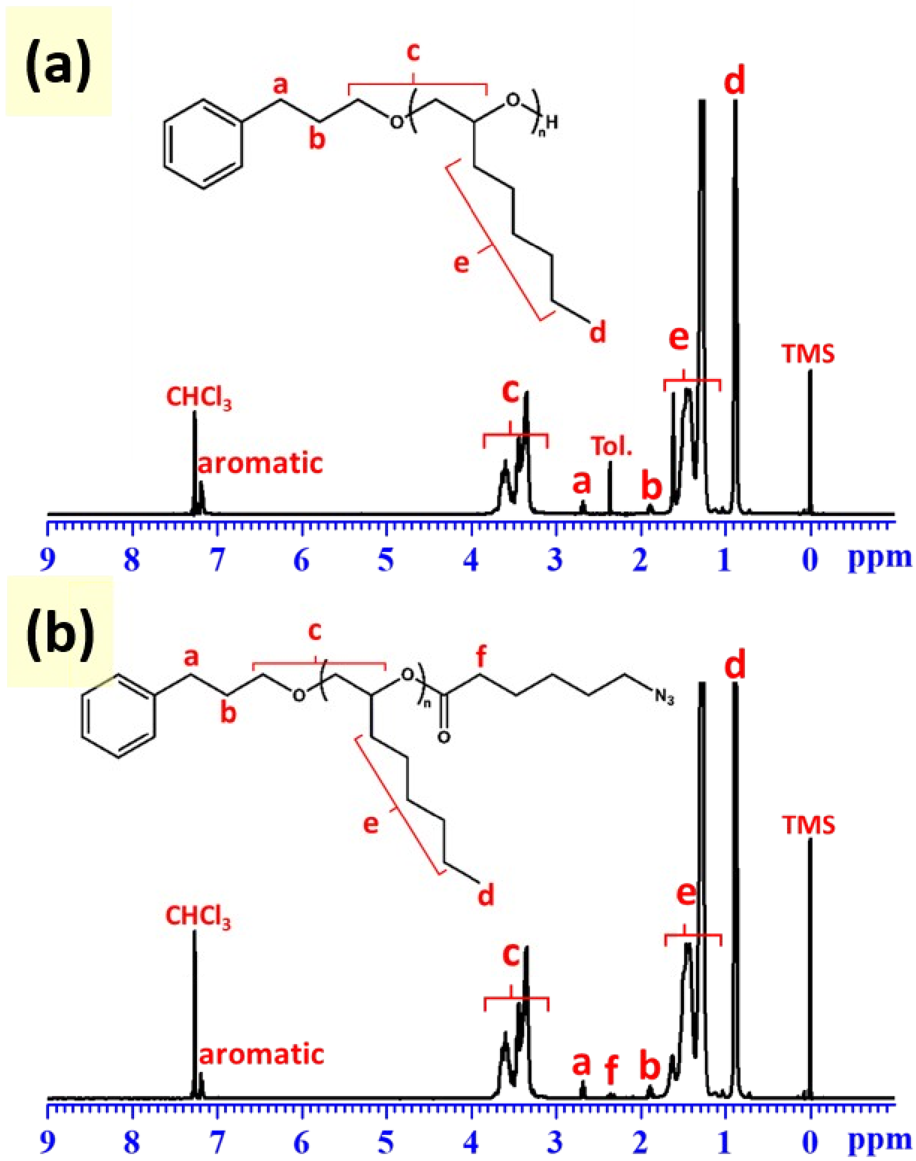

Figure S5. ^{1}H NMR spectrum of (a) POO_{36} and (b) POO_{36}-N_3.

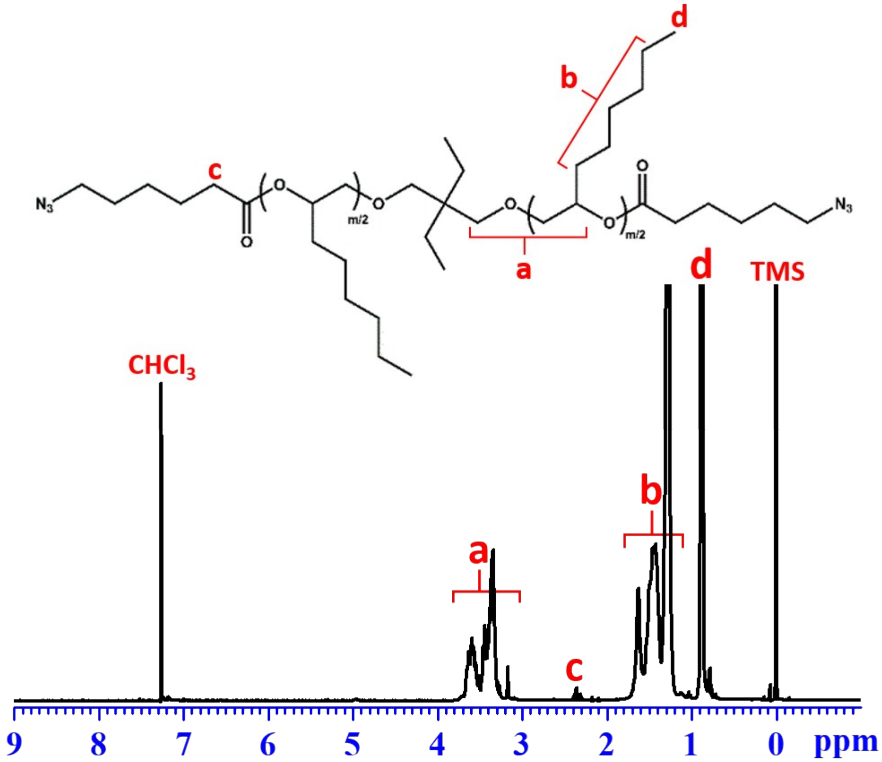

Figure S6. ^{1}H NMR spectrum of N_3-POO_{56}-N_3.

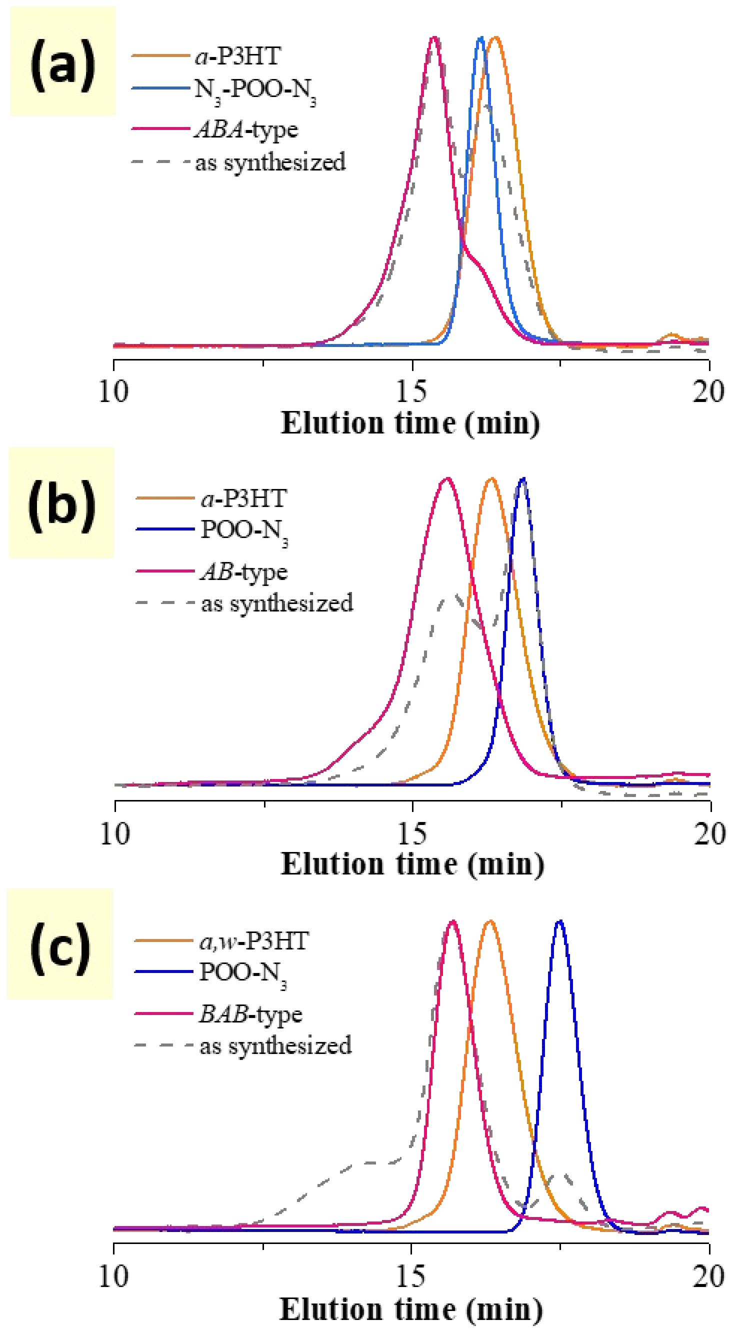

Figure S7. SEC traces of (a) ABA-type, (b) AB-type, and (c) BAB-type BCPs.

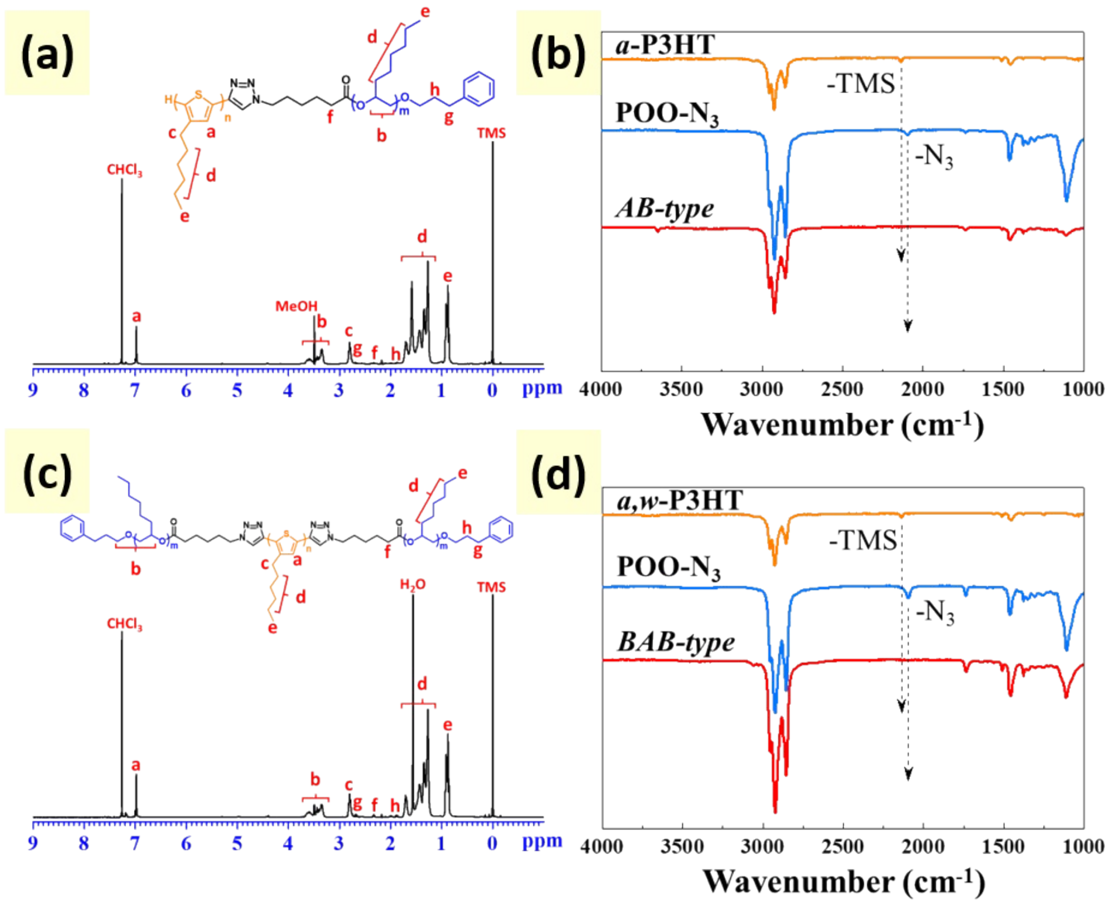

Figure S8. ^{1}H NMR and FT-IR spectra of (a-b) AB-type and (c-d) BAB-type BCPs.

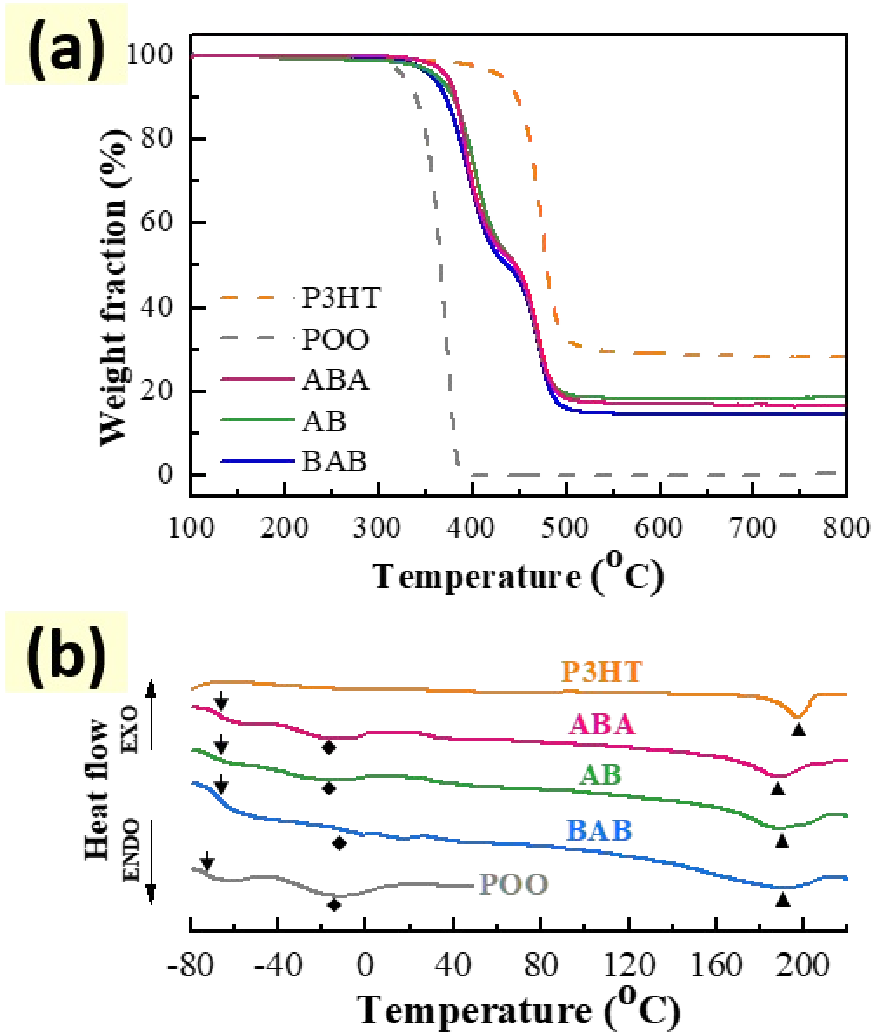

Figure S9. (a) TGA curves and (b) DSC traces of the P3HT, POO, and synthesized block copolymers.

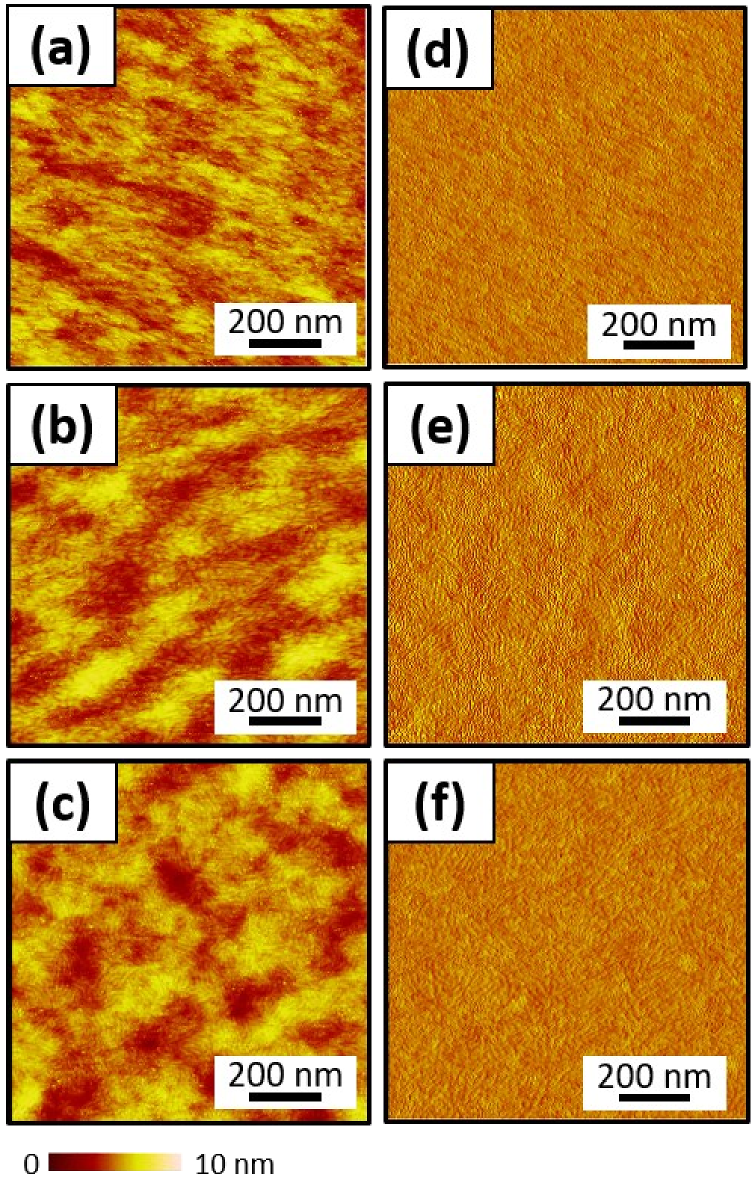

Figure S10. Tapping mode AFM topographies (left) and phase images (right) of as-cast thin films. (a, d) ABA-type, (b, e) AB-type, and (c, f) BAB-type BCPs.

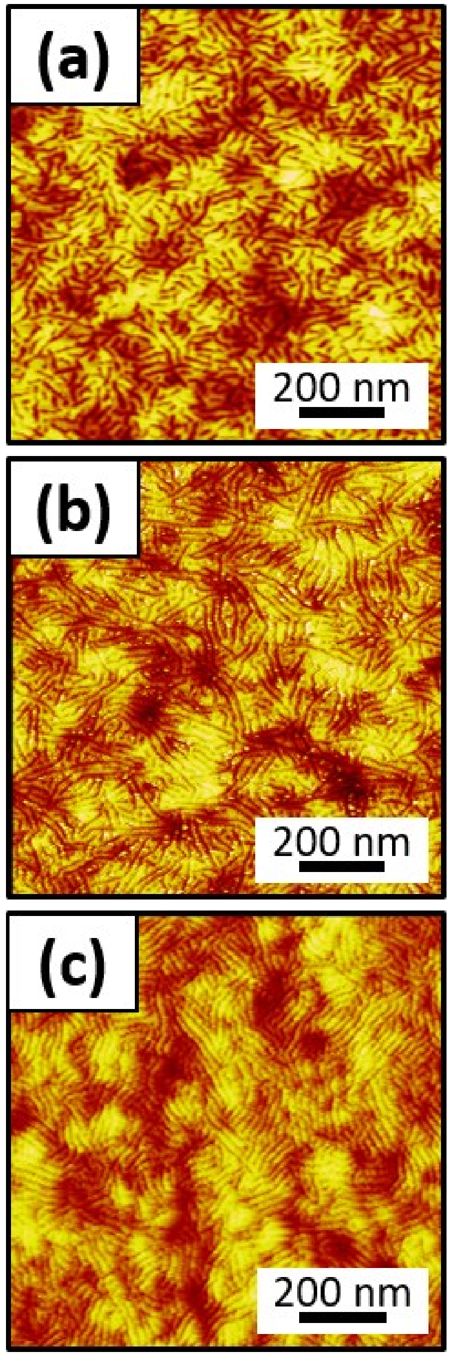

Figure S11. Tapping mode AFM topographies of annealed thin films. (a) ABA-type, (b) AB-type, and (c) BAB-type BCPs.

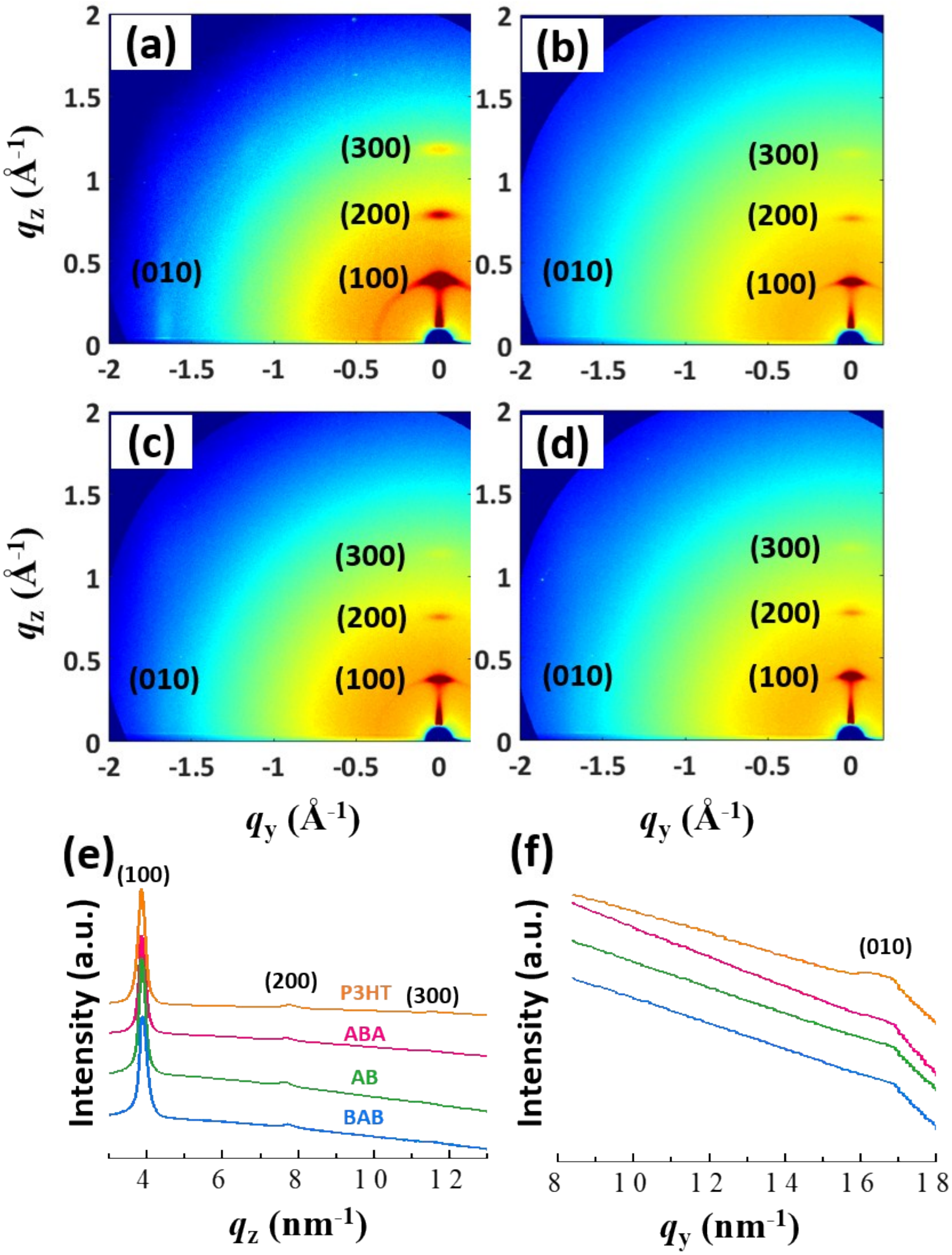

Figure S12. 2D GIWAXS patterns of annealed thin films. (a) P3HT, (b) ABA-type, (c) AB-type, and (d) BAB-type BCPs. And 1D line-cut of each polymers in the direction of (e) out-plane and (f) in-plane.

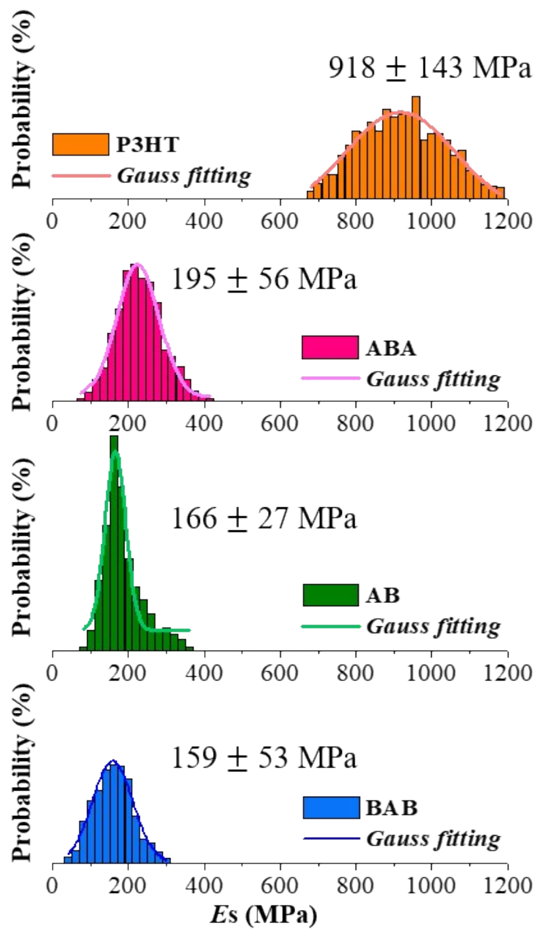

Figure S13. The distribution of the elastic moduli (E_s) of studied polymers.

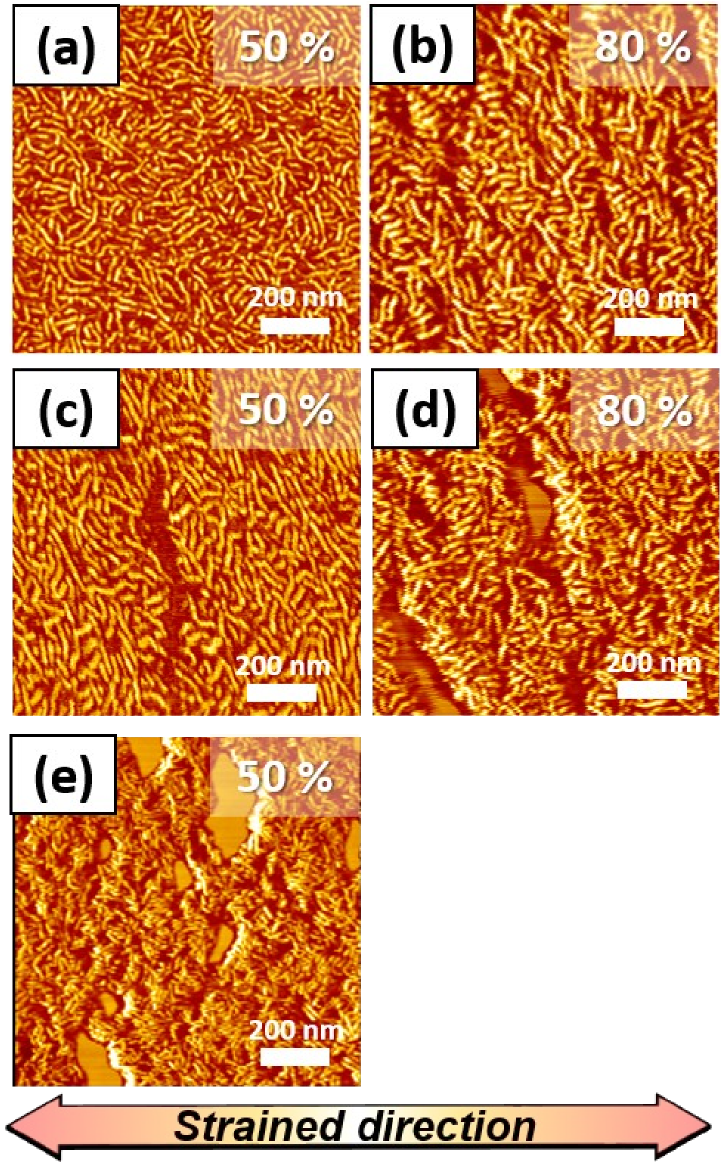

Figure S14. Tapping mode AFM phase images of thin films under various tensile strains. (a-b) ABA-type, (c-d) AB-type, and (e) BAB-type BCPs.

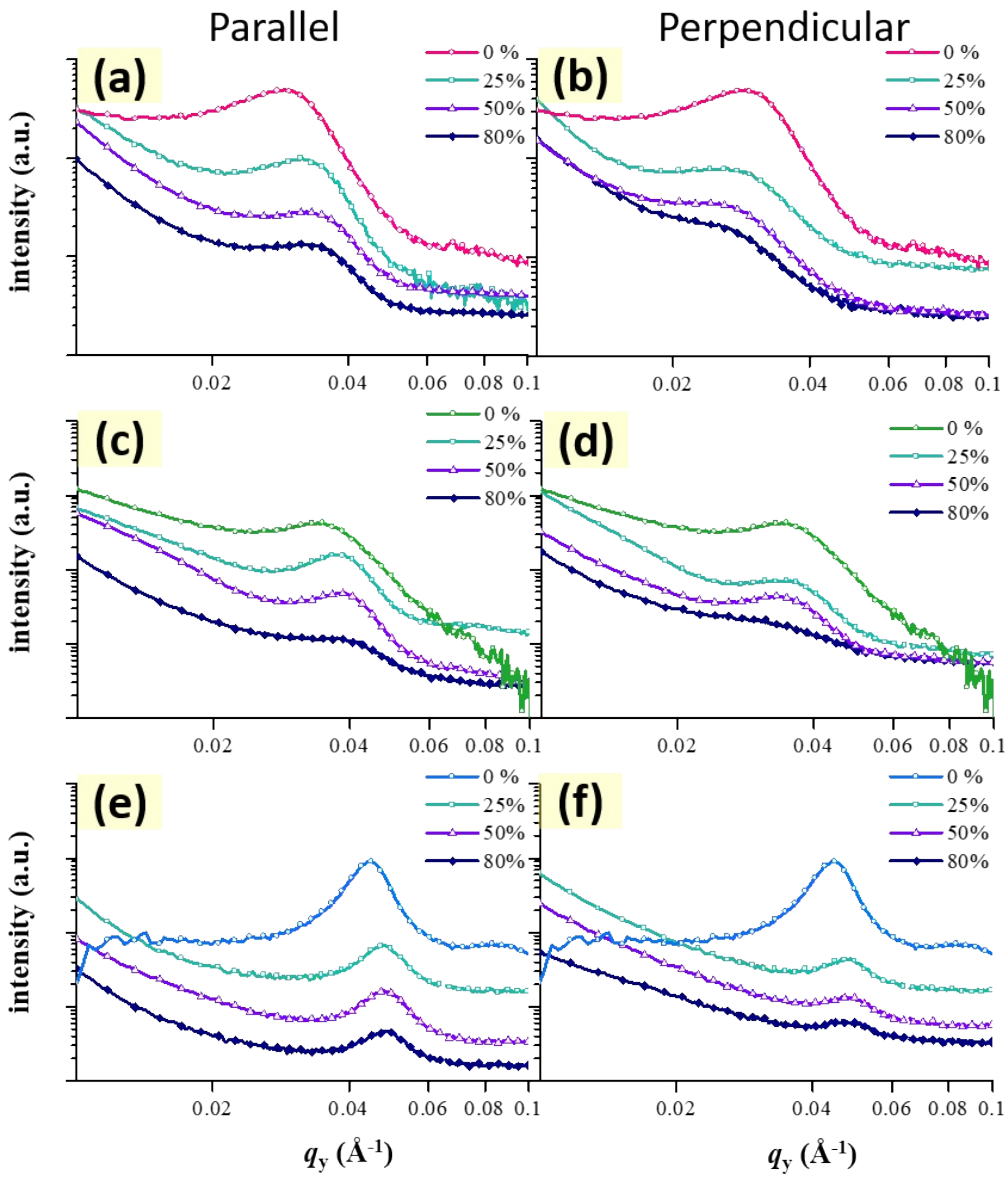

Figure S15. 1D GISAXS profiles of thin films under varying strains. (a-b) ABA-type, (c-d) AB-type, and (e-f) BAB-type BCPs. Note that the incident X-ray light is set to be perpendicular and parallel to the stretching direction.

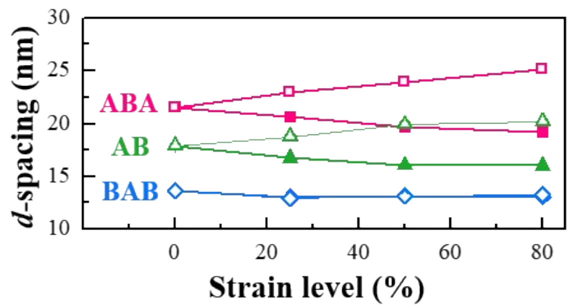

Figure S16. The *d*-spacing of the polymer thin films under varying strains. Note that the incident X-ray light is set to be perpendicular (hollowed) and parallel (filled) to the stretching direction.

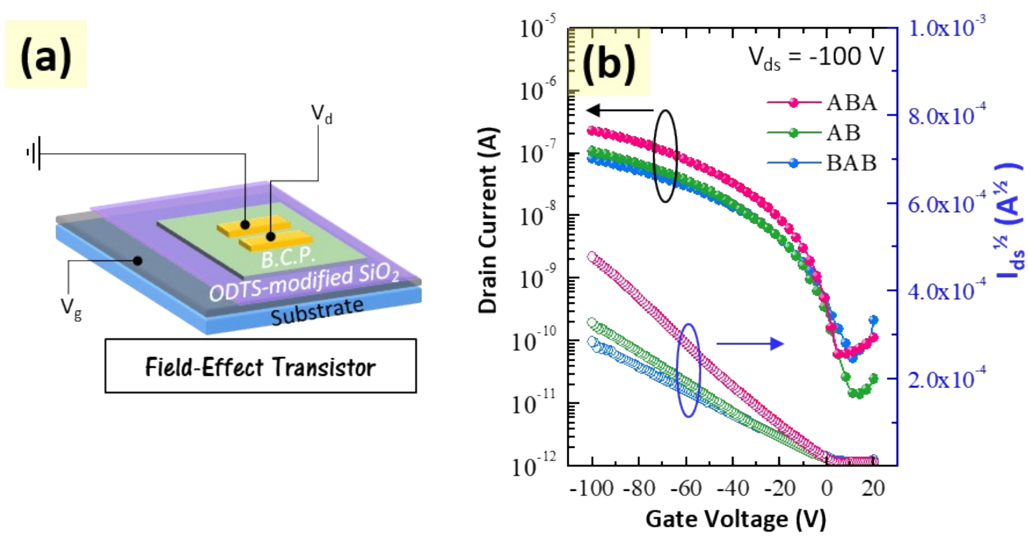

Figure S17. (a) Configuration of bottom-gate top-contact field effect transistor. (b) the FET electrical characterization of studied block copolymers.

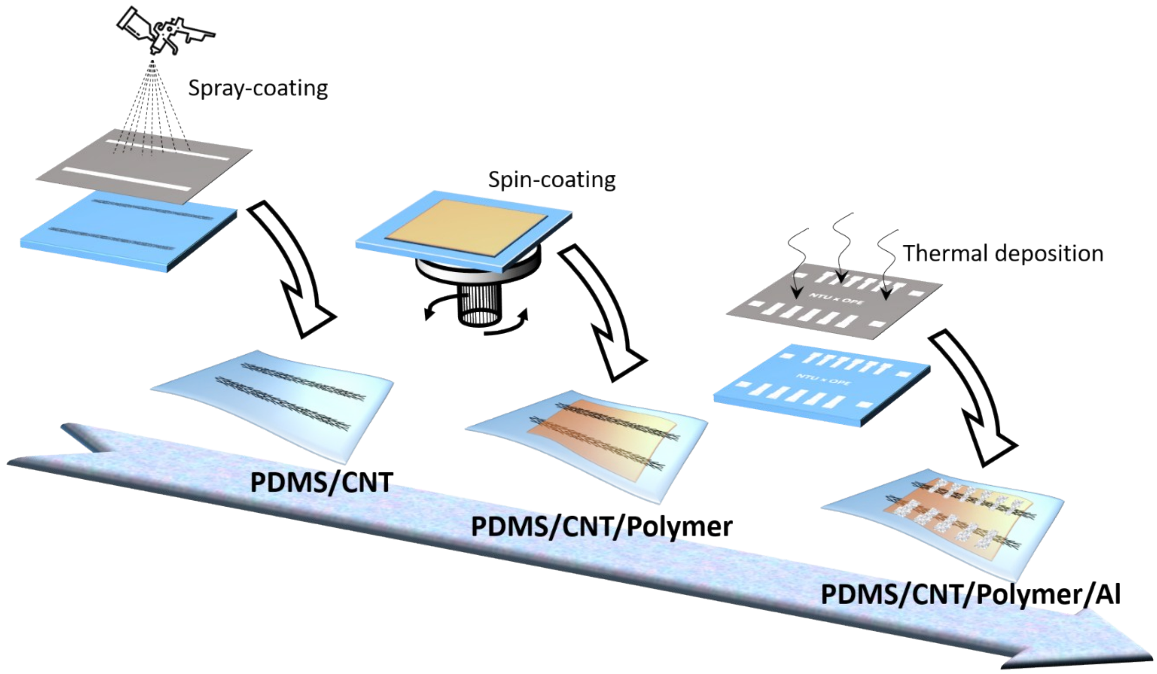

Figure S18. Schematically illustration of fabrication the stretchable resistive memory devices.

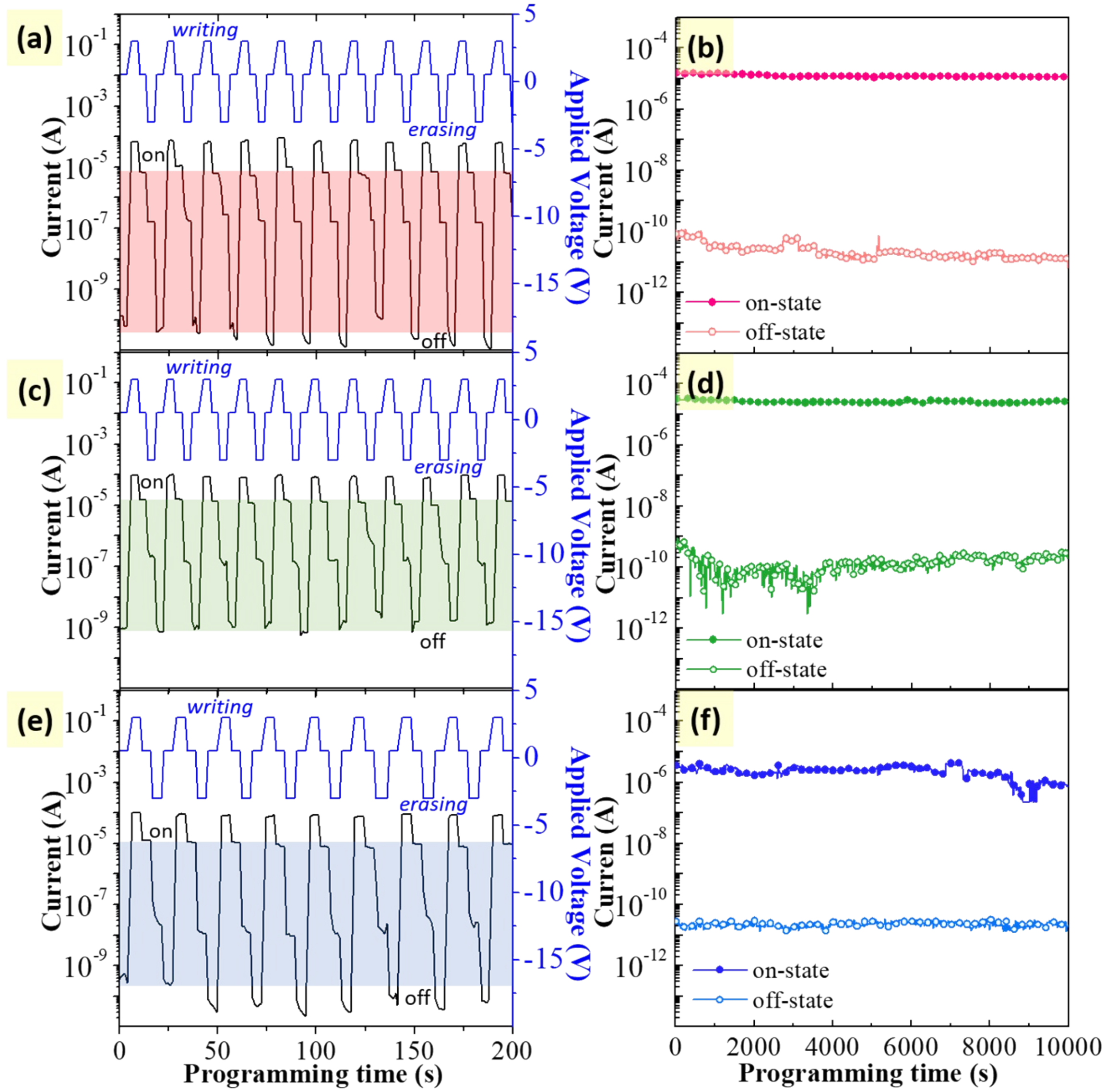

Figure S19. The write-read-erase-read (W-R-E-R) cycles and retention time curves of (a-b) ABA-type, (c-d) AB-type, and (e-f) BAB-type based-memory devices.

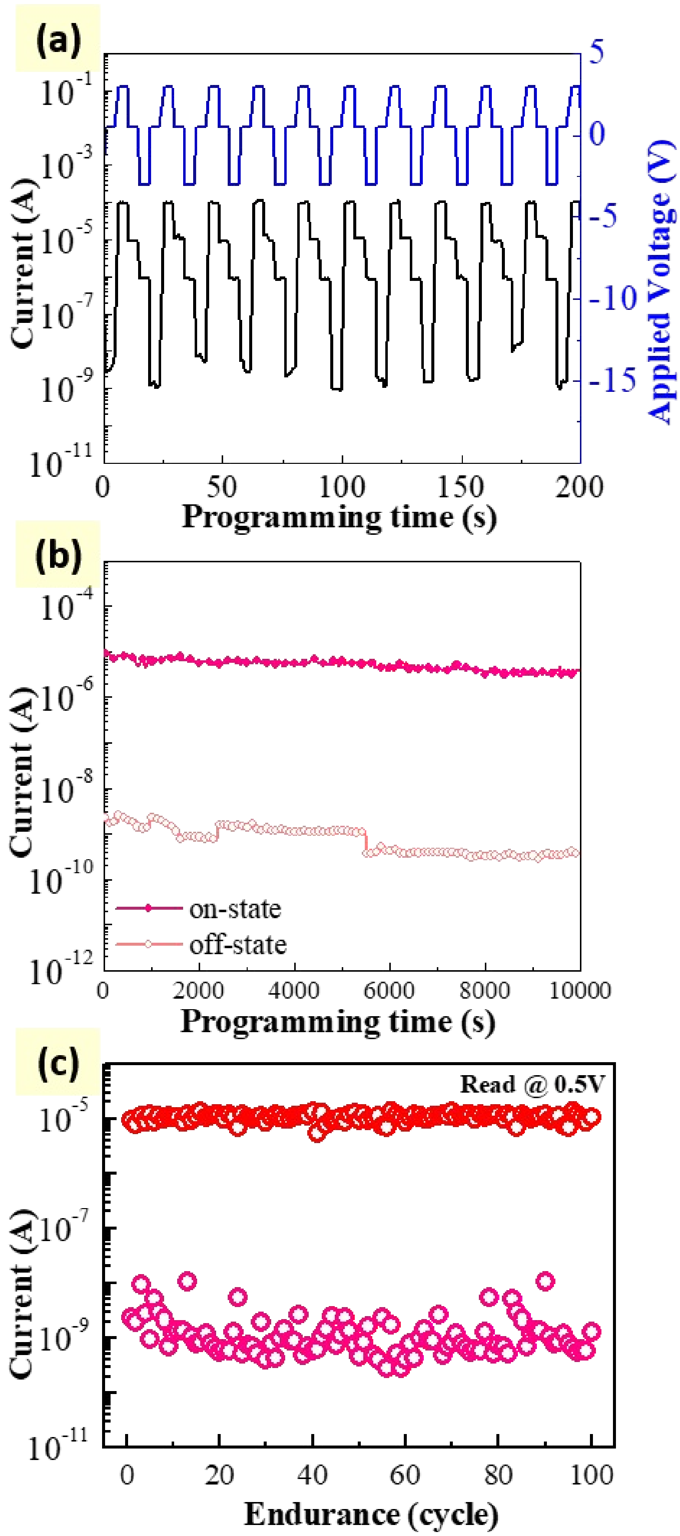

Figure S20. The (a) write-read-erase-read (W-R-E-R) cycles, (b) retention time curves, and (c) endurance of WRER cycles of ABA-type BCP thin films under 80% tensile strain.

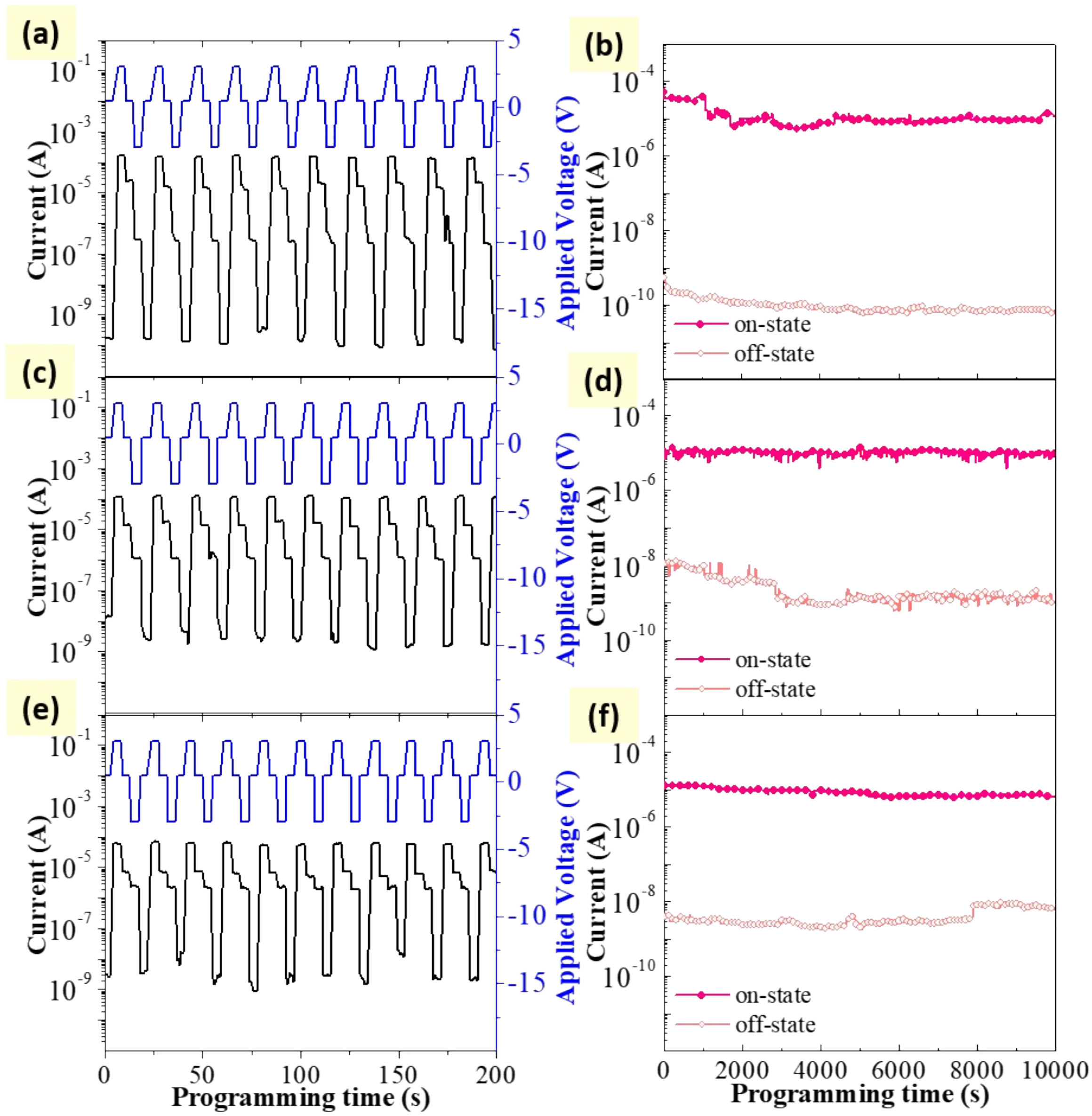

Figure S21. The W-R-E-R cycles and retention time curves of ABA-type based memory devices after cycling stretching (50% strain) for (a-b) 100 times, (c-d) 200 times, and (e-f) 500 times.

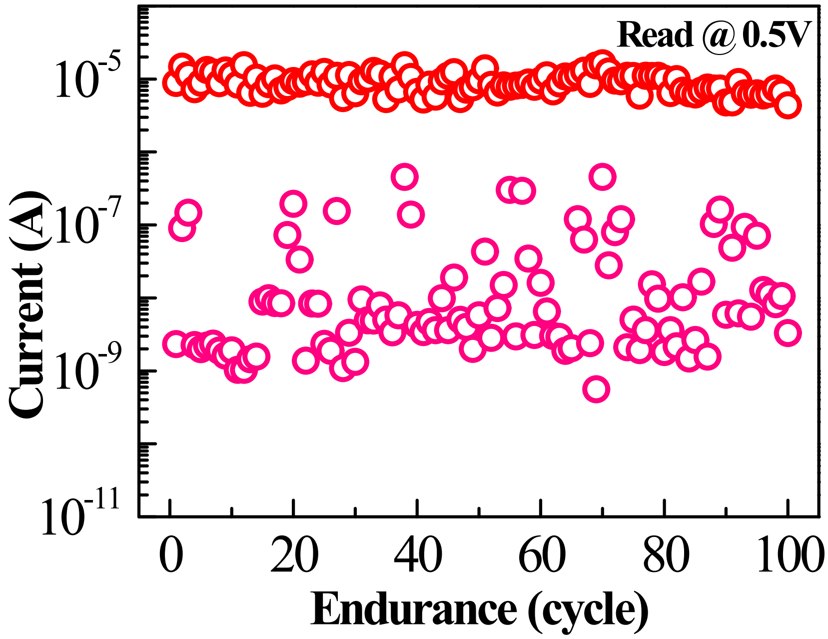

Figure S22. The endurance of WRER cycles of ABA-type memory device after 500 times of cycling stretching (50% strain).

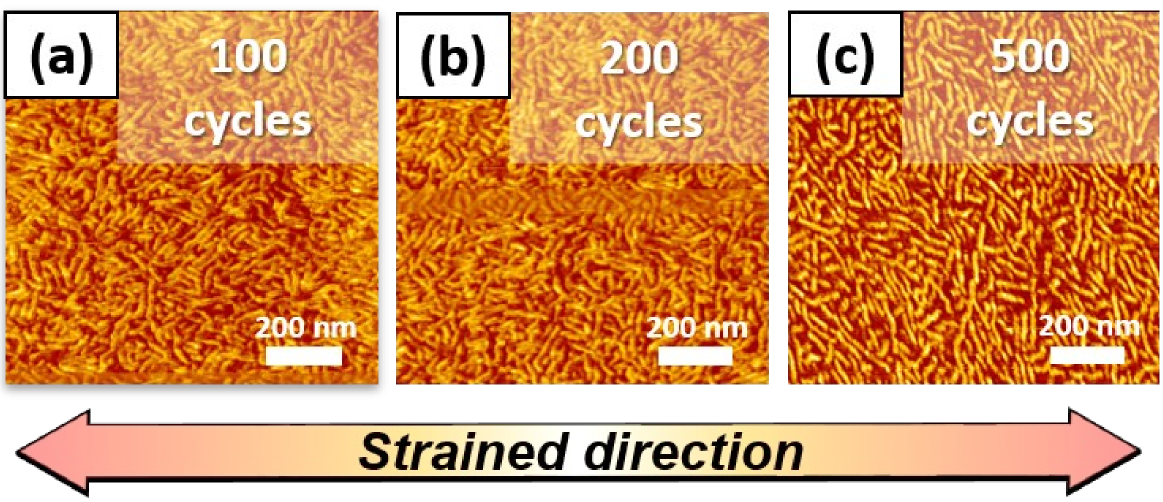

Figure S23. Tapping mode AFM phase images of ABA-type BCP thin films after varying cycling stretching (50% strain).